

# 4

## Ray theory: Travel times

Seismic ray theory is analogous to optical ray theory and has been applied for over 100 years to interpret seismic data. It continues to be used extensively today, owing to its simplicity and applicability to a wide range of problems. These applications include most earthquake location algorithms, body-wave focal mechanism determinations, and inversions for velocity structure in the crust and mantle. Ray theory is intuitively easy to understand, simple to program, and very efficient. Compared to more complete solutions, it is relatively straightforward to generalize to three-dimensional velocity models. However, ray theory also has several important limitations. It is a high-frequency approximation, which may fail at long periods or within steep velocity gradients, and it does not easily predict any “non-geometrical” effects, such as head waves or diffracted waves. The ray geometries must be completely specified, making it difficult to study the effects of reverberation and resonance due to multiple reflections within a layer.

In this chapter, we will be concerned only with the timing of seismic arrivals, deferring the consideration of amplitudes and other details to later. This narrow focus is nonetheless very useful for many problems; a significant fraction of current research in seismology uses only travel time information. The theoretical basis for much of ray theory is derived from the *eikonal equation* (see Appendix C); however, because these results are not required for most applications we do not describe them here.

### 4.1 Snell's law

Consider a plane wave, propagating in material of uniform velocity  $v$ , that intersects a horizontal interface (Fig. 4.1).

The wavefronts at time  $t$  and time  $t + \Delta t$  are separated by a distance  $\Delta s$  along the ray path. The ray angle from the vertical,  $\theta$ , is termed the incidence angle. This

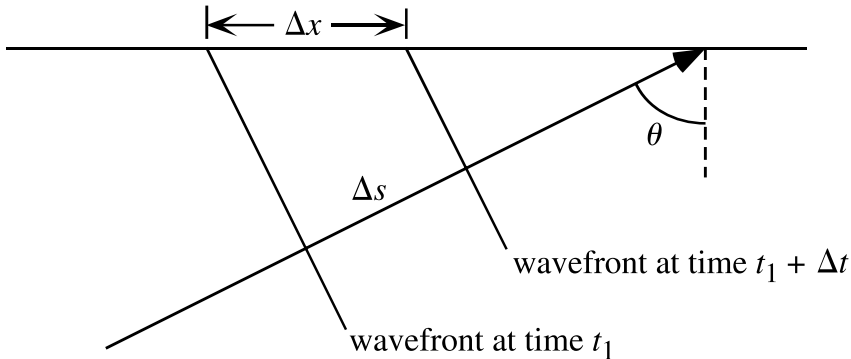


**Figure 4.1** A plane wave incident on a horizontal surface. The ray angle from vertical is termed the incidence angle  $\theta$ .

angle relates  $\Delta s$  to the wavefront separation on the interface,  $\Delta x$ , by

$$\Delta s = \Delta x \sin \theta. \quad (4.1)$$

Since  $\Delta s = v\Delta t$ , we have

$$v\Delta t = \Delta x \sin \theta \quad (4.2)$$

or

$$\frac{\Delta t}{\Delta x} = \frac{\sin \theta}{v} = u \sin \theta \equiv p, \quad (4.3)$$

where  $u$  is the *slowness* ( $u = 1/v$  where  $v$  is velocity) and  $p$  is termed the *ray parameter*. If the interface represents the free surface, note that by timing the arrival of the wavefront at two different stations, we could directly measure  $p$ . The ray parameter  $p$  represents the apparent slowness of the wavefront in a horizontal direction, which is why  $p$  is sometimes called the *horizontal slowness* of the ray.

Now consider a downgoing plane wave that strikes a horizontal interface between two homogeneous layers of different velocity and the resulting transmitted plane wave in the lower layer (Fig. 4.2). If we draw wavefronts at evenly spaced times along the ray, they will be separated by different distances in the different layers, and we see that the ray angle at the interface must change to preserve the timing of the wavefronts across the interface.

In the case illustrated the top layer has a slower velocity ( $v_1 < v_2$ ) and a correspondingly larger slowness ( $u_1 > u_2$ ). The ray parameter may be expressed in terms of the slowness and ray angle from the vertical within each layer:

$$p = u_1 \sin \theta_1 = u_2 \sin \theta_2. \quad (4.4)$$

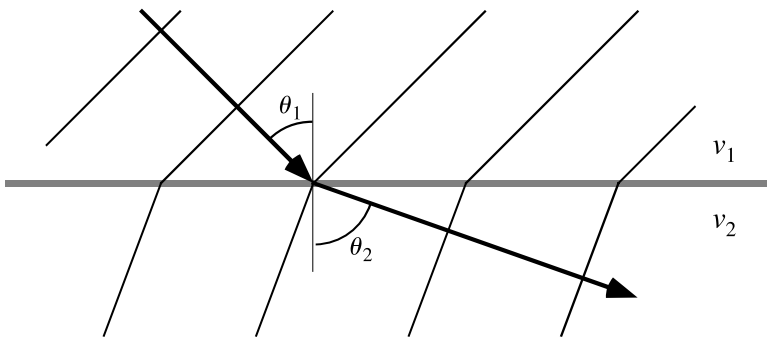


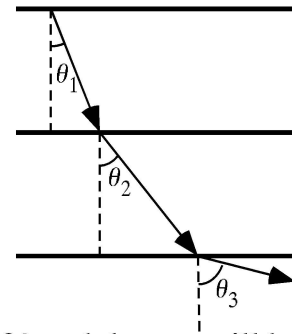
**Figure 4.2** A plane wave crossing a horizontal interface between two homogeneous half-spaces. The higher velocity in the bottom layer causes the wavefronts to be spaced further apart.

Notice that this is simply the seismic version of Snell's law in geometrical optics. Equation (4.4) may also be obtained from *Fermat's principle*, which states that the travel time between two points must be stationary (usually, but not always, the minimum time) with respect to small variations in the ray path. Fermat's principle itself can be derived from applying variational calculus to the eikonal equation (e.g., Aki and Richards, 2002, pp. 89–90).

## 4.2 Ray paths for laterally homogeneous models

In most cases the compressional and shear velocities increase as a function of depth in the Earth. Suppose we examine a ray traveling downward through a series of layers, each of which is faster than the layer above. The ray parameter  $p$  remains constant and we have

$$p = u_1 \sin \theta_1 = u_2 \sin \theta_2 = u_3 \sin \theta_3. \quad (4.5)$$



If the velocity continues to increase,  $\theta$  will eventually equal  $90^\circ$  and the ray will be traveling horizontally.

This is also true for continuous velocity gradients (Fig. 4.3). If we let the slowness at the surface be  $u_0$  and the *takeoff angle* be  $\theta_0$ , we have

$$u_0 \sin \theta_0 = p = u \sin \theta. \quad (4.6)$$

When  $\theta = 90^\circ$  we say that the ray is at its *turning point* and  $p = u_{tp}$ , where  $u_{tp}$  is the slowness at the turning point. Since velocity generally increases with depth in Earth, the slowness *decreases* with depth. Smaller ray parameters are more steeply dipping at the surface, will turn deeper in Earth, and generally travel farther. In these examples with horizontal layers or vertical velocity gradients,  $p$  remains

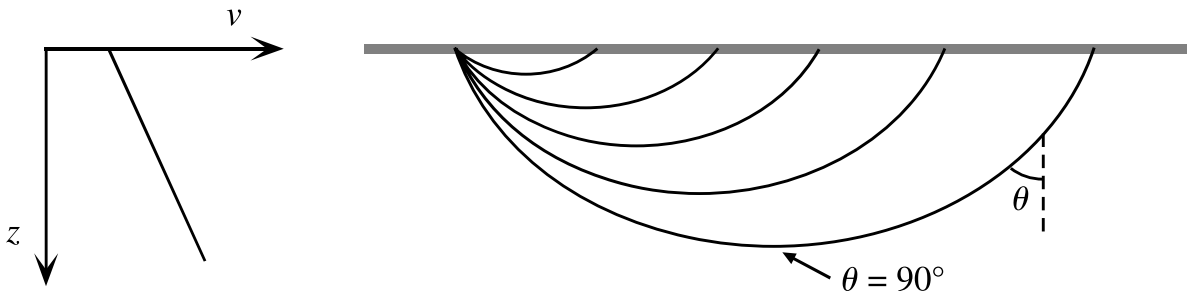


**Figure 4.3** Ray paths for a model that has a continuous velocity increase with depth will curve back toward the surface. The ray turning point is defined as the lowermost point on the ray path, where the ray direction is horizontal and the incidence angle is  $90^\circ$ .

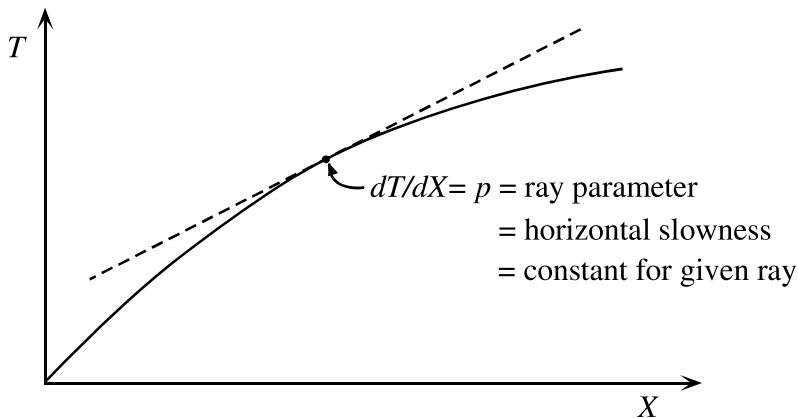
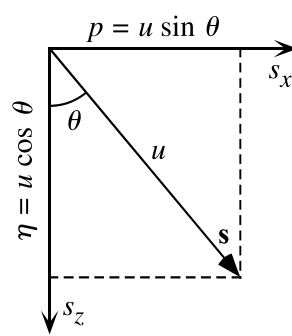


**Figure 4.4** A travel time curve for a model with a continuous velocity increase with depth. Each point on the curve results from a different ray path; the slope of the travel time curve,  $dT/dX$ , gives the ray parameter.

constant along the ray path. However, if lateral velocity gradients or dipping layers are present, then  $p$  will change along the ray path.

In a model in which velocity increases with depth,<sup>1</sup> the *travel time curve*, a plot of the first arrival time versus distance, will look like Figure 4.4. Note that  $p$  varies along the travel time curve; a different ray is responsible for the “arrival” at each distance  $X$ . At any point along a ray, the slowness vector  $s$  can be resolved into its horizontal and vertical components. The length of  $s$  is given by  $u$ , the local slowness. The horizontal component,  $s_x$ , of the



<sup>1</sup> Observant readers may notice that our coordinate system has now flipped so that  $z$  is no longer pointing upward as it did in Chapters 2 and 3, but rather points downward so that depths from the surface are positive. Both conventions are often used in seismology, depending upon which is more convenient.

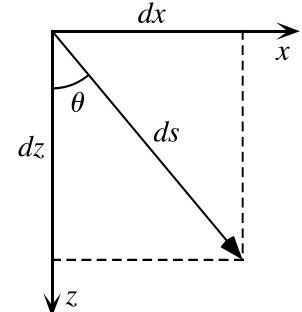
slowness is the ray parameter  $p$ . In an analogous way, we may define the vertical slowness  $\eta$  by

$$\eta = u \cos \theta = (u^2 - p^2)^{1/2}. \quad (4.7)$$

At the turning point,  $p = u$  and  $\eta = 0$ .

Let us now develop integral expressions to compute travel time and distance along a particular ray. Consider a segment of length  $ds$  along a ray path. From the geometry we have

$$\frac{dx}{ds} = \sin \theta, \quad \frac{dz}{ds} = \cos \theta = (1 - \sin^2 \theta)^{1/2}. \quad (4.8)$$



Since  $p = u \sin \theta$ , we may write

$$\frac{dx}{ds} = \frac{p}{u}, \quad \frac{dz}{ds} = (1 - p^2/u^2)^{1/2} = u^{-1}(u^2 - p^2)^{1/2}. \quad (4.9)$$

From the chain rule

$$\frac{dx}{dz} = \frac{dx}{ds} \frac{ds}{dz} = \frac{dx/ds}{dz/ds} = \frac{p}{u} \frac{u}{(u^2 - p^2)^{1/2}} = \frac{p}{(u^2 - p^2)^{1/2}}. \quad (4.10)$$

This can be integrated to obtain  $x$ :

$$x(z_1, z_2, p) = p \int_{z_1}^{z_2} \frac{dz}{(u^2(z) - p^2)^{1/2}}. \quad (4.11)$$

If we let  $z_1$  be the free surface ( $z_1 = 0$ ) and  $z_2$  be the turning point  $z_p$ , the distance  $x$  from the surface source to the surface point over the turning point is

$$x(p) = p \int_0^{z_p} \frac{dz}{(u^2(z) - p^2)^{1/2}}. \quad (4.12)$$

Because the ray is symmetric about the turning point, the total distance  $X(p)$  from surface source to surface receiver is just twice this expression, that is,

$$X(p) = 2p \int_0^{z_p} \frac{dz}{(u^2(z) - p^2)^{1/2}}. \quad (4.13)$$

In a similar way, we can derive an expression for the travel time  $t(p)$ :

$$dt = u \, ds, \quad dt/ds = u, \quad (4.14)$$

$$\frac{dt}{dz} = \frac{dt}{ds} \frac{ds}{dz} = \frac{dt/ds}{dz/ds} = \frac{u^2}{(u^2(z) - p^2)^{1/2}}, \quad (4.15)$$

and we obtain

$$t(p) = \int_0^{z_p} \frac{u^2(z)}{(u^2(z) - p^2)^{1/2}} dz. \quad (4.16)$$

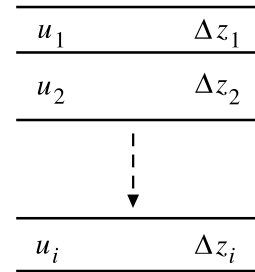
This gives the travel time from the surface to the turning point,  $z_p$ . The total surface-to-surface travel time,  $T(p)$ , is given by

$$T(p) = 2 \int_0^{z_p} \frac{u^2(z)}{(u^2(z) - p^2)^{1/2}} dz. \quad (4.17)$$

Equations (4.13) and (4.17) are suitable for a model in which  $u(z)$  is a continuous function of depth.

The simplest velocity models are specified as a stack of homogeneous layers. In this case the integrals for  $X$  and  $T$  become summations:

$$X(p) = 2p \sum_i \frac{\Delta z_i}{(u_i^2 - p^2)^{1/2}}, \quad u_i > p, \quad (4.18)$$



and

$$T(p) = 2 \sum_i \frac{u_i^2 \Delta z_i}{(u_i^2 - p^2)^{1/2}}, \quad u_i > p. \quad (4.19)$$

Note that we sum over the layers from the top downward until the layer slowness is less than the ray parameter; we don't want  $(u^2(z) - p^2)^{1/2}$  to become imaginary.

### 4.2.1 Example: Computing $X(p)$ and $T(p)$

Consider a homogeneous three-layer model with 3 km layer thicknesses and velocities 4, 6 and 8 km/s for the top, middle and bottom layers, respectively. What is the surface-to-surface distance and travel time for a ray with  $p = 0.15$  s/km? We first convert the velocities to slownesses and obtain  $u_1 = 0.25$ ,  $u_2 = 0.167$ , and  $u_3 = 0.125$  s/km. We also have  $\Delta z_1 = \Delta z_2 = \Delta z_3 = 3$  km.

In equations (4.18) and (4.19), note that  $u$  is only greater than  $p$  for layers 1 and 2. This means that the ray will pass through these layers but will be reflected off the top of layer 3. We thus have:

$$\begin{aligned} X(p) &= 2p \frac{\Delta z_1}{(u_1^2 - p^2)^{1/2}} + 2p \frac{\Delta z_2}{(u_2^2 - p^2)^{1/2}} \\ &= \frac{2 \cdot 3 \cdot 0.15}{(0.25^2 - 0.15^2)^{1/2}} + \frac{2 \cdot 3 \cdot 0.15}{(0.1677^2 - 0.15^2)^{1/2}} \\ &= 16.9 \text{ km} \end{aligned}$$

and

$$\begin{aligned} T(p) &= 2 \frac{u_1^2 \Delta z_1}{(u_1^2 - p^2)^{1/2}} + 2 \frac{u_2^2 \Delta z_2}{(u_2^2 - p^2)^{1/2}} \\ &= \frac{2 \cdot 3 \cdot 0.25^2}{(0.25^2 - 0.15^2)^{1/2}} + \frac{2 \cdot 3 \cdot 0.167^2}{(0.1677^2 - 0.15^2)^{1/2}} \\ &= 4.17 \text{ s} \end{aligned}$$

The ray travels for 4.17 s and hits the surface 16.9 km from the source.

### 4.2.2 Ray tracing through velocity gradients

When velocity gradients are present, (4.18) and (4.19) are not very convenient since a “staircase” model with a large number of homogeneous layers must be evaluated to give accurate results. A better strategy is to parameterize the velocity model at a number of discrete points in depth and evaluate the integrals (4.12) and (4.16) by assuming an appropriate interpolation function between the model points. For a linear velocity gradient between model points of the form  $v(z) = a + bz$ , the slope of the gradient,  $b$ , between  $v_1(z_1)$  and  $v_2(z_2)$  is given by

$$b = \frac{v_2 - v_1}{z_2 - z_1}. \quad (4.20)$$

Evaluating the integrals for  $t(p)$  and  $x(p)$ , one can then obtain (e.g., Chapman *et al.*, 1988)

$$x(p) = \frac{\eta}{b u p} \left|_{u_2}^{u_1} \right. \quad (4.21)$$

and

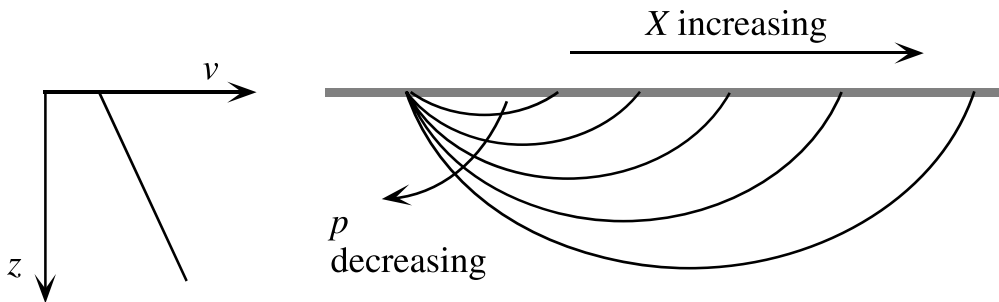
$$t(p) = \frac{1}{b} \left[ \ln \left( \frac{u + \eta}{p} \right) - \frac{\eta}{u} \right] \Bigg|_{u_2}^{u_1} + px(p), \quad (4.22)$$

where the vertical slowness  $\eta = (u^2 - p^2)^{1/2}$ . If the ray turns within the layer, then there is no contribution to these integrals from the lower point. A computer subroutine that uses these expressions to compute  $x(p)$  and  $t(p)$  for a layer with a linear velocity gradient is provided in Appendix D; this is needed in some of the Exercises.

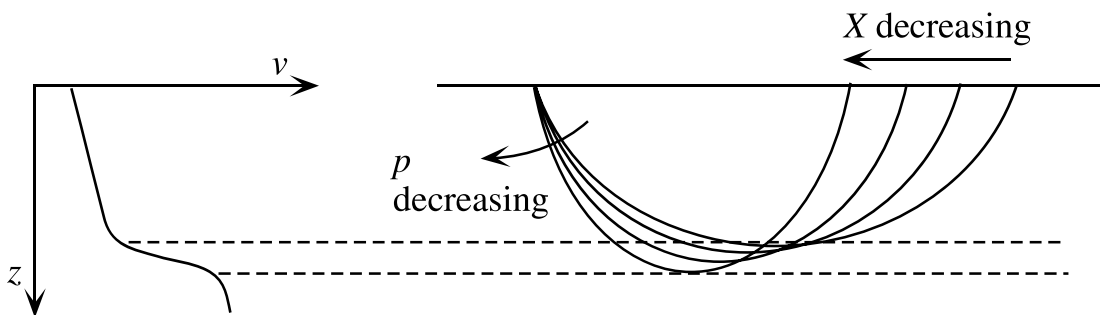
### 4.3 Travel time curves and delay times

---

Generally in the Earth,  $X(p)$  will increase as  $p$  decreases; that is, as the takeoff angle decreases, the range increases:



In this case the derivative  $dX/dp$  is negative. When  $dX/dp < 0$ , we say that this *branch* of the travel time curve is *prograde*. Occasionally, because of a rapid velocity transition in the Earth,  $dX/dp > 0$ , and the rays turn back on themselves:



When  $dX/dp > 0$  the travel time curve is termed *retrograde*. The transition from prograde to retrograde and back to prograde generates a *triplication* in the travel time curve (Fig. 4.5). The endpoints on the triplication are termed *caustics*. These

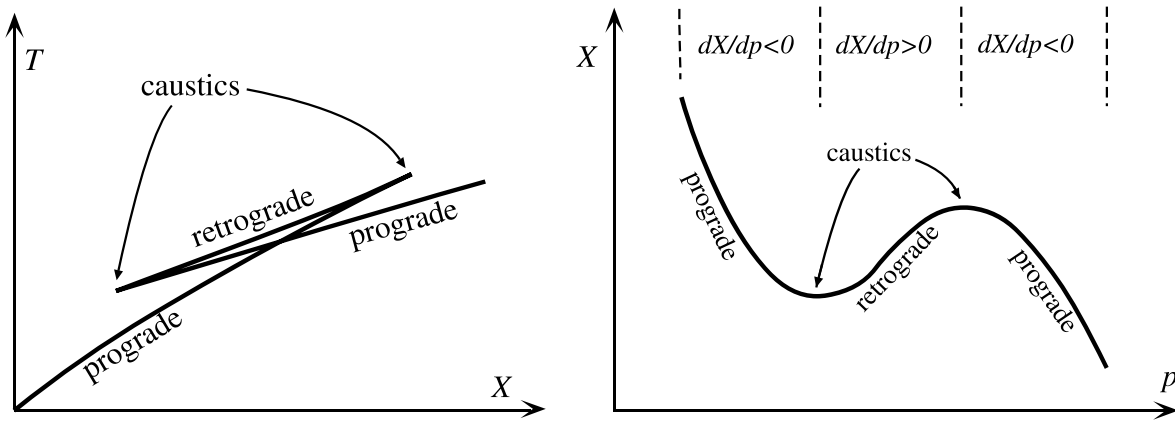


**Figure 4.5** A triplication in the travel time curve and the corresponding  $X(p)$  curve resulting from a steep velocity increase.

are the points where  $dX/dp = 0$ . Energy is focused to these points since rays at different takeoff angles arrive at the same range (as we shall see later, geometrical ray theory predicts infinite amplitude at these points!). The triplication may be “unraveled” by considering the  $X(p)$  function.

At large values of  $p$  the rays turn at shallow depths and travel only short distances. As the ray parameter decreases, the turning point depth increases and the range,  $X$ , increases. When the turning points enter the steep velocity gradient,  $X$  begins decreasing with decreasing  $p$ . Once the rays break through the steep velocity gradient and turn in the more shallow gradient below,  $X$  once again increases with decreasing  $p$ . The caustics are the stationary points on the  $X(p)$  curve. However, it should be noted that sharp changes in the velocity gradient (i.e., discontinuities in  $dv/dz$ ) will produce sharp bends in the  $X(p)$  curve so that it will not always have the smooth appearance shown in Figure 4.5. In particular, local maxima or minima in  $X(p)$  may be present where  $dX/dp$  is discontinuous and a caustic does not occur.

### 4.3.1 Reduced velocity

Travel time curves can often be seen in more detail if they are plotted using a *reduction velocity* that is subtracted from the travel times (Figure 4.6). In this case the time scale is shifted an amount equal to the range divided by the reducing velocity. Velocities that are equal to the reduction velocity will plot as horizontal lines, and a greatly expanded time scale becomes possible.

### 4.3.2 The $\tau(p)$ function

The function  $X(p)$  is more nicely behaved than  $T(X)$  since it does not cross itself (there is a single value of  $X$  for each value of  $p$ ), but the inverse function  $p(X)$  is

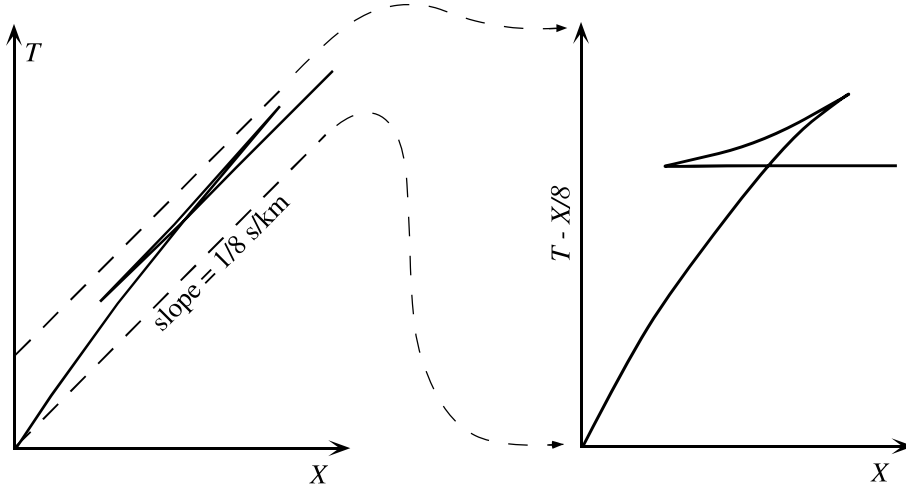


**Figure 4.6** A reduction velocity can be used to expand the time scale to show more detail in travel time curves.

multivalued. An even nicer function is the combination

$$\tau(p) = T(p) - pX(p), \quad (4.23)$$

where  $\tau$  is called the *delay time*. It can be calculated very simply from (4.13) and (4.17):

$$\begin{aligned} \tau(p) &= 2 \int_0^{z_p} \left[ \frac{u^2}{(u^2 - p^2)^{1/2}} - \frac{p^2}{(u^2 - p^2)^{1/2}} \right] dz \\ &= 2 \int_0^{z_p} (u^2(z) - p^2)^{1/2} dz \\ &= 2 \int_0^{z_p} \eta(z) dz. \end{aligned} \quad (4.24)$$

For our simple layered medium, we have

$$\tau(p) = 2 \sum_i \left( u_i^2 - p^2 \right)^{1/2} \Delta z_i = 2 \sum_i \eta_i \Delta z_i, \quad u_i > p. \quad (4.25)$$

Consider a point on a travel time curve  $t(x)$  at distance  $X$  and time  $T$  (Fig. 4.7). The equation of the straight line tangent to the travel time curve is  $t = T + p(x - X)$ . At  $x = 0$ ,  $t = T - pX = \tau(p)$ , so the intercept of the line is  $\tau(p)$  while the slope is  $p$ . The slope of the  $\tau$  versus  $p$  curve is

$$\frac{d\tau}{dp} = \frac{d}{dp} 2 \int_0^{z_p} (u^2 - p^2)^{1/2} dz = -2p \int_0^{z_p} \frac{dz}{(u^2 - p^2)^{1/2}} \quad (4.26)$$

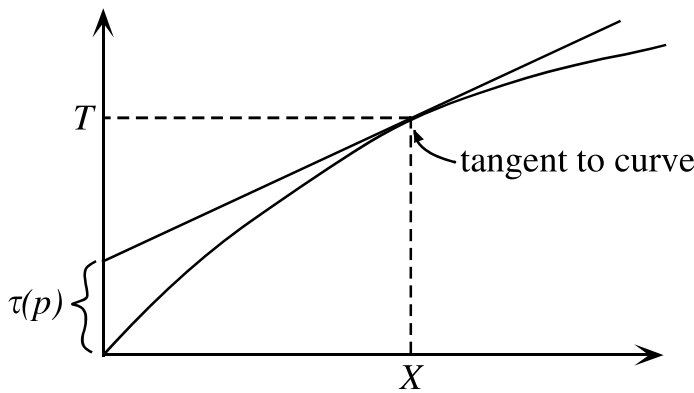


**Figure 4.7** The delay time,  $\tau(p) = T - pX$ , is given by the intercept of the tangent to the travel time curve.

and thus

$$\frac{d\tau}{dp} = -X(p). \quad (4.27)$$

The slope of the  $\tau(p)$  curve is  $-X$ . Because  $X \geq 0$ , the  $\tau(p)$  curve is always decreasing, or *monotonically decreasing*. The  $\tau(p)$  curve remains monotonically decreasing ( $d\tau/dp < 0$ ) even in the presence of a triplication in the  $T(X)$  curve. The second derivative of  $\tau$  is simply

$$\frac{d^2\tau}{dp^2} = \frac{d}{dp}(-X) = -\frac{dX}{dp}. \quad (4.28)$$

The  $\tau(p)$  curve is concave upward for a prograde branch and concave downward for a retrograde branch (Fig. 4.8). The functions  $X(p)$ ,  $T(p)$ , and  $\tau(p)$  are “proper” in that they are single valued.  $T(X)$ , on the other hand, is not a proper function since

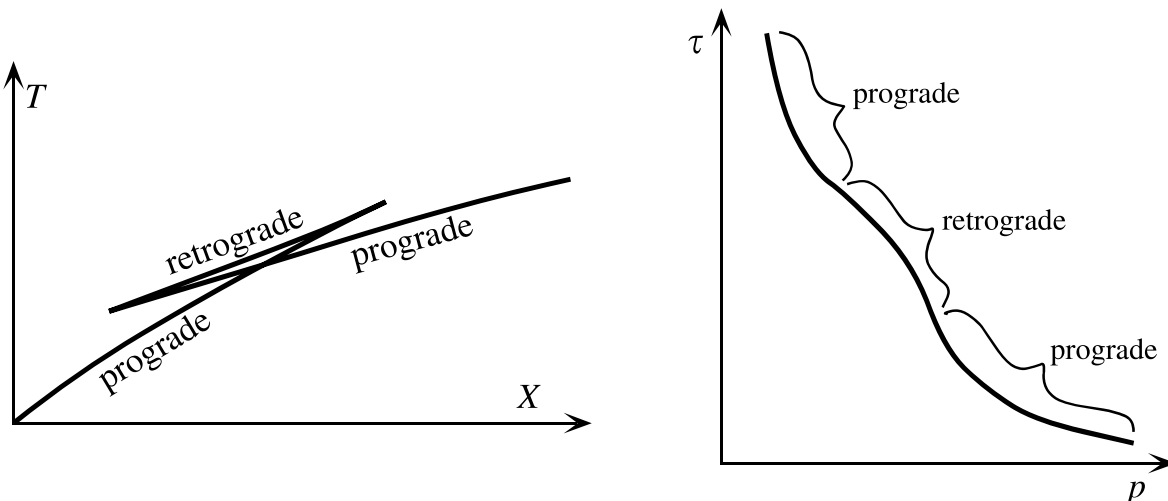


**Figure 4.8** The  $\tau(p)$  function “unravels” triplications in travel time curves. Prograde branches have concave upward  $\tau(p)$  curves; retrograde branches have concave downward  $\tau(p)$  curves.

it will generally be multivalued. This difference means that  $\tau(p)$  data, if available, are generally easier to interpret than  $T(X)$  data. We shall see in the next chapter that working in the  $\tau(p)$  domain has advantages in computing velocity versus depth functions from travel time data.

## 4.4 Low-velocity zones

In all of the examples plotted above, we have assumed that velocity always increases with depth. However, occasionally we will encounter the case where velocity decreases with depth, creating a *low-velocity zone* (LVZ). The outstanding example in Earth is the core, where the  $P$  velocity drops from about 14 km/s in the lowermost mantle to 8 km/s in the outermost core. There is also considerable evidence for a LVZ in the upper mantle, at least in shear velocity, within the asthenosphere (about 80 to 200 km depth). Within the negative velocity gradient at the top of the LVZ, the rays are bent downward (Fig. 4.9). Note that no rays originating at the surface

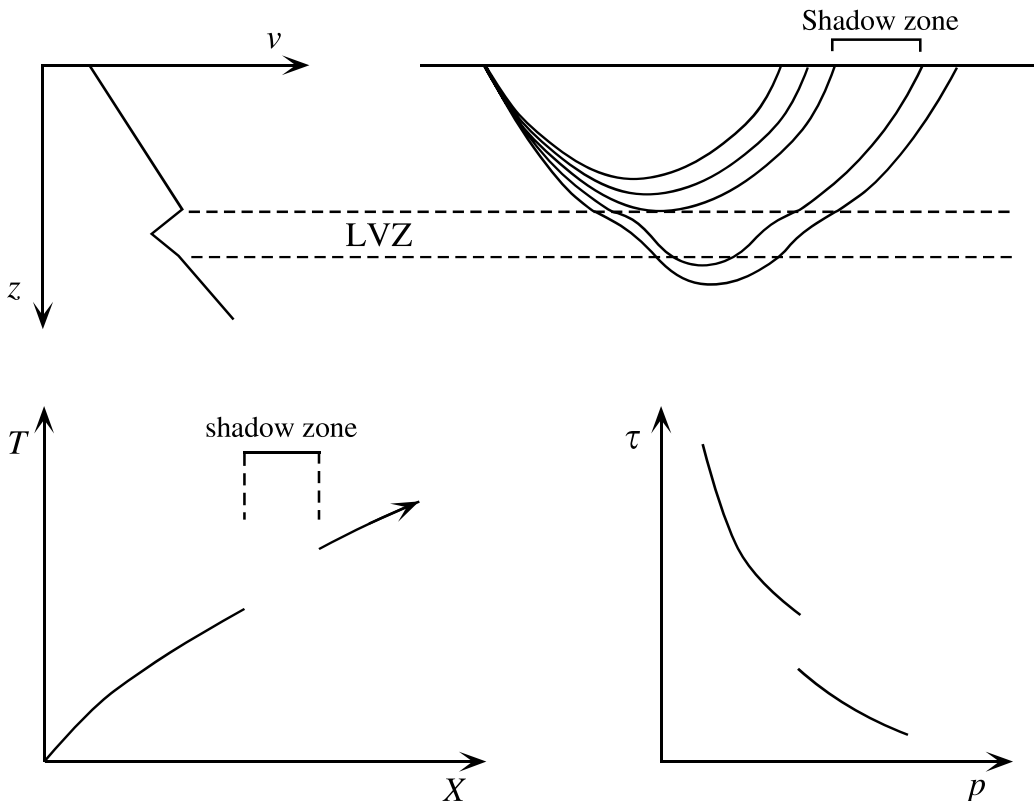


**Figure 4.9** A low velocity zone (LVZ) results from a velocity decrease with depth. Rays curve downward as the velocity decreases, creating a shadow zone on the surface and gaps in the  $T(X)$  and  $\tau(p)$  curves.

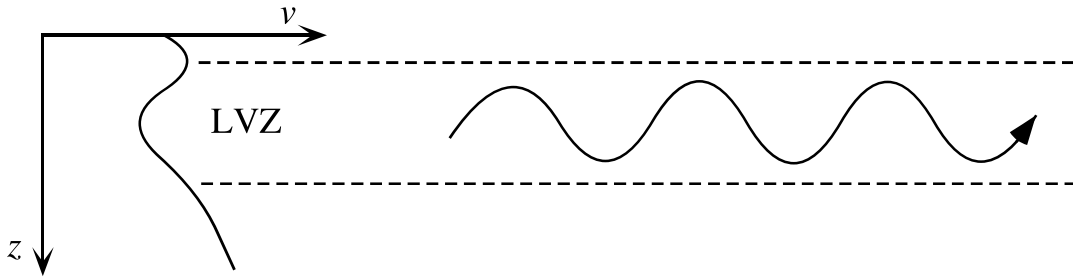


**Figure 4.10** A low-velocity zone (LVZ) can trap waves, creating a wave guide.

can turn within the LVZ itself. Rays with horizontal slownesses corresponding to values within the LVZ turn above the zone. Only when the ray parameter becomes small enough do rays enter the LVZ. These rays then pass through the low velocity zone and turn in the region below the LVZ in which velocities are once again higher than any velocities in the overlying material.

The existence of a low velocity zone creates a gap, termed a *shadow zone*, in both the  $T(X)$  and  $\tau(p)$  curves. The absence of rays turning within the LVZ often makes the velocity structure within low velocity zones difficult to determine. A related phenomenon arises when rays originate within a low velocity zone. In this case, some rays are trapped within the LVZ and are forever curving back in toward the velocity minimum (Fig. 4.10). The LVZ acts as a *wave guide* and, in cases of low attenuation, seismic energy can propagate very long distances. The most notable example of a wave guide in Earth is the sound channel in the ocean. Acoustic waves trapped within the sound channel can be detected over distances of thousands of kilometers.

## 4.5 Summary of 1-D ray tracing equations

Let us now review the important equations for ray tracing in laterally homogeneous Earth models. First, the ray parameter or horizontal slowness  $p$  is defined by several expressions:

$$p = u(z) \sin \theta = \frac{dT}{dX} = u_{tp} = \text{constant for given ray}, \quad (4.29)$$

where  $u = 1/v$  is the slowness,  $\theta$  is the ray incidence angle (from vertical),  $T$  is the travel time,  $X$  is the horizontal range, and  $u_{tp}$  is the slowness at the ray turning

point. We also defined the vertical slowness

$$\eta = (u^2 - p^2)^{1/2} \quad (4.30)$$

and integral expressions for the surface-to-surface travel time  $T(p)$ , range  $X(p)$ , and delay time  $\tau(p)$ :

$$T(p) = 2 \int_0^{z_p} \frac{u^2(z)}{(u^2(z) - p^2)^{1/2}} dz = 2 \int_0^{z_p} \frac{u^2(z)}{\eta} dz, \quad (4.31)$$

$$X(p) = 2p \int_0^{z_p} \frac{dz}{(u^2(z) - p^2)^{1/2}} = 2p \int_0^{z_p} \frac{dz}{\eta}, \quad (4.32)$$

and

$$\tau(p) = 2 \int_0^{z_p} (u^2(z) - p^2)^{1/2} dz = 2 \int_0^{z_p} \eta(z) dz, \quad (4.33)$$

where  $z_p$  is the turning point depth ( $p = u$  at the turning point). We also have

$$\tau(p) = T(p) - pX(p) \quad (4.34)$$

and

$$X(p) = -\frac{d\tau}{dp}. \quad (4.35)$$

The  $T(X)$ ,  $X(p)$ ,  $\tau(p)$  functions can be quite sensitive to even small changes in the velocity-depth model. Figure 4.11 illustrates the relationships between these functions for some simple models. These examples demonstrate that even slight changes in seismic velocity gradients can have large effects on the resulting ray paths. It is also apparent that many if not most triplications will not have the simple form illustrated in Figure 4.5 where the  $X(p)$  curve has smooth maxima and minima. Discontinuities in the vertical velocity gradient produce sharp bends in the  $X(p)$  function, and triplications can exist without formal caustics at their endpoints where  $dX/dp = 0$ . Staircase models are interesting because all of their ray paths involve reflections off the top of layers and thus are on retrograde branches, connected by straight lines on the  $T(X)$  curve that define the first arrivals. These first arrivals represent head waves traveling along the top of each layer. They have zero energy in geometrical ray theory but more complete synthetic seismogram calculations show that they do produce observable arrivals, although generally of low amplitude.

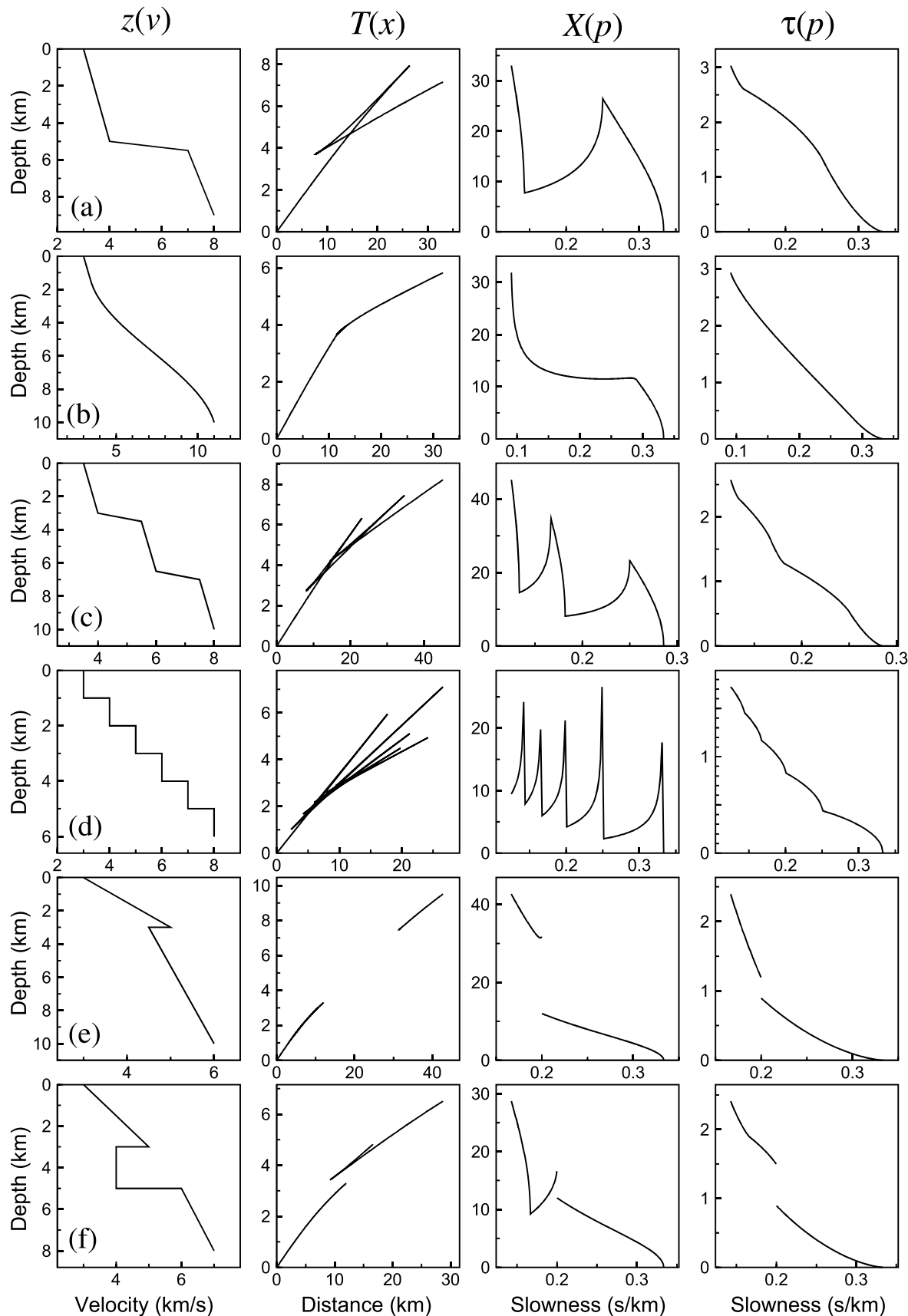


**Figure 4.11** The  $T(X)$ ,  $X(p)$ ,  $\tau(p)$  curves for assorted velocity-depth models ( $z(v)$ ), illustrating (a) a simple triplication, (b) a velocity model that focuses many of the rays to a single  $T(X)$  point, (c) a double triplication, (d) a staircase model, (e) a low-velocity zone, and (f) a low-velocity zone with a sharp velocity jump. Note:  $T$  and  $\tau$  are in s,  $x$  and  $z$  are in km.